ELSEVIER

Journal of Nuclear Materials 290–293 (2001) 464–468

journal of nuclear materials

www.elsevier.nl/locate/jnucmat

Origins and spatial distributions of core fueling in the DIII-D tokamak

L.W. Owen [a,*], R.J. Colchin [a], R. Maingi [a], M.E. Fenstermacher [b], T.N. Carlstrom [c], R.J. Groebner [c]

[a] Oak Ridge National Laboratory, P.O. Box 2009, Oak Ridge, TN 37831-8072, USA
[b] Lawrence Livermore National Laboratory, Livermore, CA, USA
[c] General Atomics, P.O. Box 85608, San Diego, CA 92186-9784, USA

Abstract

Analysis of DIII-D discharge data with fluid plasma and Monte Carlo neutrals transport codes reveals that core particle fueling stays relatively constant between the L-mode and the ELM-free H-mode phase immediately following the L–H transition. This indicates that in the ELM-free phase nearly all of the increase in plasma electron density comes from a decrease in the cross-field transport rate and an increase in the impurity influx. This result differs from conclusions of previous work in that the effects of the thinner H-mode scrape-off-layer do not appear to be as important in a plasma that is fueled primarily from divertor recycling as would be expected if the fueling from limiter recycling were dominant. In both L-mode and H-mode the calculated core particle confinement times are less than, but within 50% of, the corresponding energy confinement times.

Keywords: 2D Model; DIII-D; Monte Carlo simulation; Particle confinement time; Recycling; SOL transport

1. Introduction

The effects of neutrals on plasma properties and confinement quality has been extensively studied both theoretically and experimentally. These studies are motivated by the need to understand where neutrals originate, by what processes they are transported into the plasma, their role as the plasma fueling source, their effects upon the dynamics and transport of the plasma, etc. One focus of the theoretical studies has been the effects of neutrals on the power threshold for the transition from the low (L) to high (H) confinement mode [1–3]. Experiments showed that access to the H-mode requires reduction in recycling through careful wall conditioning [4]. That wall conditioning affects the neutral density in the plasma was inferred only indirectly from measurements of neutral pressure outside the plasma. A recent study from the DIII-D tokamak used data-constrained 2-D plasma and neutrals modeling to conclude that the neutral density in the core plasma near the *X*-point was high enough to affect flow damping in the shear layer by the mechanism of charge-exchange friction [5]. The conclusion from this study was uncertain because the neutral density itself was unmeasured. A recently developed multi-diagnostic technique [6] to measure neutral densities in the *X*-point region of DIII-D, where the core particle fueling is largest, has shown that the *X*-point neutral densities predicted in [5] for low power L-mode discharges were indeed correct.

The focus of the work reported here and a key element in the studies reported in [5,7] is determination of the fueling of the core plasma by neutrals recycling from the divertor. The analysis technique is discussed in [5,7] and will be only briefly outlined here. Typically available DIII-D diagnostic data that are used to constrain the model are main chamber electron density and temperature profiles from Thomson scattering, divertor D_α

* Corresponding author. Tel.: +1-423 574 0634; fax: +1-423 574 1191.
E-mail address: lwo@ornl.gov (L.W. Owen).

0022-3115/01/$ - see front matter
PII: S0022-3115(00)00582-1

emissivities from a filterscope array, ion temperatures from charge-exchange recombination (CER) spectroscopy, divertor heat flux from an IRTV camera, divertor density, temperature and ion flux at the divertor plates from embedded Langmuir probes, n_e and T_e from divertor Thomson scattering (DTS), 2-D radiation profiles, and neutral densities measured in the *X*-point region (by the method discussed in [6]). The plasma data are fit with the 2-D plasma fluid transport code B2.5 [8], and the resulting plasma parameters are used in the DEGAS Monte Carlo neutrals transport code [9] to calculate core fueling rates and neutrals distributions. In the procedure used here the plasma and neutrals codes are not linked, but satisfaction of the core particle balance equation is imposed as a necessary constraint to ensure consistency of the core fueling rate and the core ion efflux. Iteration of the B2.5 and DEGAS simulations is required in order to simultaneously satisfy the core particle balance and to fit both the plasma and neutrals data.

Data from lower single-null (LSN) DIII-D discharges in which the ion grad-B drift is toward the *X*-point are analyzed in both L-mode and H-mode phases. This paper will focus on a subset of three of the analyzed cases, namely the 3700 ms time slice in each of the discharges 96740 (L-mode, $P_h = 0.88$ MW), 96745 (H-mode, $P_h = 1.6$ MW) and 96747 (H-mode, $P_h = 2.5$ MW), where P_h is the input heating power. The *X*-point height above the divertor is approximately 0.1 m and the line-averaged density is 2.5×10^{19} m^{-3}.

The focus of this paper is on comparison of calculated neutral densities with recent measurements in L-mode and H-mode plasmas, and on using these and other measurements to benchmark core plasma fueling simulations in DIII-D. In Section 2 the neutral density measurement technique is briefly reviewed and the discharges chosen for analysis are described. Analysis results are presented and compared with the neutral density data in Section 3. Core fueling and particle confinement time calculations are discussed in Section 4.

2. Discussion of the data

In order to study core particle fueling in a variety of plasma conditions, we have analyzed three time slices in each of four discharges. One of the discharges (96333) had an L–H transition triggered by an *X*-point radius increase at constant input power. The other three discharges attained H-mode with an increase in the neutral beam power. Due to space limitations this paper will focus on a single time slice (3700 ms) from each of the three latter discharges. During these discharges the *X*-point radius was held fixed and the *X*-point height above the divertor floor was decreased at 500 ms intervals beginning at 3500 ms. In two of the discharges (96745 and 96747) the beam power was increased and the L–H transition occurred at that time as well. The third discharge of the three (96740) had no increase in beam power and remained in L-mode until very near the end. With these four discharges we are able to study the effects of input power, line-averaged density, *X*-point position, and confinement mode on core fueling and core particle confinement time.

Fig. 1 shows the time evolution of discharges 96740 and 96745; 96747 is similar to 96745 except that the L-mode phase density (before 3500 ms) is lower and the input power after 3500 ms is higher. The transition to H-mode at 3500 ms is evident in the D_α trace for 96745; during the subsequent 1 s ELM-free phase, the density increases by a factor of three. The dN/dt values estimated from these traces are shown in Table 1.

The analysis technique used here differs from that discussed in [5] only in the data that serves to constrain the analysis. Here we have, in addition, used electron density and temperature data from the DTS system and measured neutral densities in the *X*-point region. The neutral density measurement technique uses D_α data from a tangentially viewing video (TTV) camera calibrated by a vertically viewing photomultiplier [6]. Electron densities and temperatures from the DTS diagnostic are required to deduce the neutral density from the calibrated D_α. Consequently the extent of the DTS chord inside the plasma determines how deeply into the core plasma that the neutral density can be measured; the lower the *X*-point the more DTS points fall within the core plasma rather than the private flux region. For the discharges analyzed here, the DTS chord passes through that *X*-point.

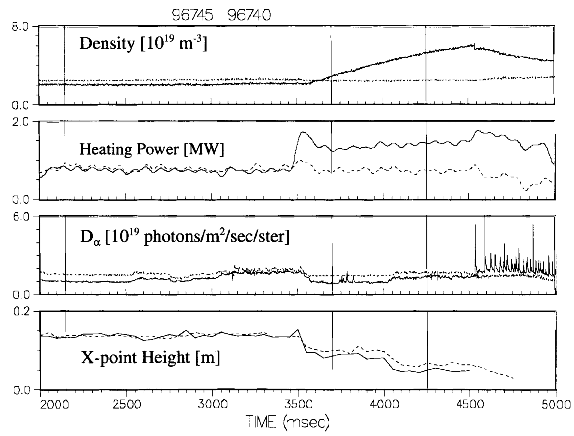

Fig. 1. Time traces of the line-averaged electron density, neutral beam heating power, D_α emissivity, and *X*-point height above the divertor floor for shots 96740 (dashed lines) and 96745 (solid lines).

Table 1
Discharge parameters and plasma/neutrals transport modeling results that demonstrate satisfaction of the core plasma particle balance equation and approximate constancy of the divertor ion fluxes and core fueling rates for L-mode and ELM-free H-mode

Discharge Time (ms)/L,H mode	96740 3700/L-mode	96745 3700/H-mode	96747 3700/H-mode
P_{sep} (MW)	0.71	0.88	1.38
Total P_{rad} (MW)	0.43	0.48	0.58
dN_e/dt (s^{-1})	0	9.4×10^{20}	0.19×10^{21}
P_{div}^{in} (MW) (exp.)	0.067	0.083	0.212
P_{div}^{in} (MW) (calc.)	0.116	0.111	0.213
P_{div}^{out} (MW) (exp.)	0.304	0.297	0.346
P_{div}^{out} (MW) (calc.)	0.291	0.336	0.357
I_{div}^{in} (s^{-1}) (calc.)	6.46×10^{21}	6.88×10^{21}	6.53×10^{21}
I_{div}^{out} (s^{-1}) (calc.)	9.66×10^{21}	1.05×10^{22}	8.71×10^{21}
B2.5 core efflux (s^{-1})	3.15×10^{21}	2.44×10^{21}	1.96×10^{21}
DEGAS core fuel. (s^{-1})	3.11×10^{21}	3.15×10^{21}	2.74×10^{21}
NBI fuel. rate (s^{-1})	3.56×10^{19}	1.60×10^{20}	2.97×10^{20}
τ_E (s)	0.18	0.31	0.28
τ_p (s)	0.15	0.21	0.25

3. Comparisons of data and simulation results

At the 3700 ms time slice all of the discharge data mentioned in Section 1, except for divertor Langmuir probe (LP) measurements, are available and used to constrain the analyses of 96740, 96745 and 96747. Divertor LP data from earlier in the discharge is used for the L-mode in 96740 since the density is nearly constant. For the H-mode time slices the measured divertor D_α emissivities are the principal diagnostic data used in the determination of the total divertor recycling flux. The *X*-point neutral density and core fueling rate depend directly upon the divertor recycling flux; hence, accurate determination of this flux is a key to fitting the neutrals data and satisfying core particle balance. The fit to the D_α emissivity data shown in Fig. 2 for 96745 is typical of the H-mode analysis results. For low power L-mode, we fit both the inner and outer divertor LP ion flux profiles, but only the outer D_α emissivity. The calculated inner divertor D_α profile is typically lower than the measurements; this effect is thought to be related to the model description of the detached or partially detached state of the inner divertor. Although not shown the n_e and T_e profiles from Thomson scattering, T_i from CER, and the divertor IRTV data are also fit very well by the model. In order to balance the power crossing the separatrix and that measured by the IRTV and bolometers, the model uses hydrogenic radiation enhancement factors to simulate impurity radiation [10].

In a previous study [5] that focused entirely on analysis of low power L-mode plasmas, DTS data were fit reasonably well but were not used to constrain the model, as has been done here. We find in this work that calculated core neutral densities and core fueling

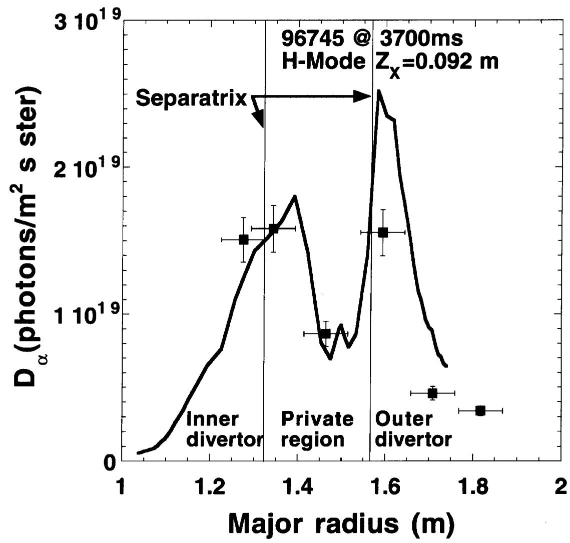

Fig. 2. H-mode D_α emissivity data for shot 96745 is compared to results of B2.5/DEGAS transport simulations.

rates in L-mode are less sensitive to the fit to the DTS data than are those in H-mode. In fact it is not possible to fit the measured H-mode core neutral density unless the measured DTS n_e and T_e in the core plasma are reproduced. The reason for this is related to the differences in the L-and H-mode core plasma profiles just inside the separatrix. Ionization and charge-exchange at the H-mode pedestal have a large effect on the neutral density profile and must be accurately modeled. The model fits to the measured atomic neutral density data in L- and H-mode are illustrated in Figs. 3(a) and (b). At the *X*-point the neutral density in H-mode is

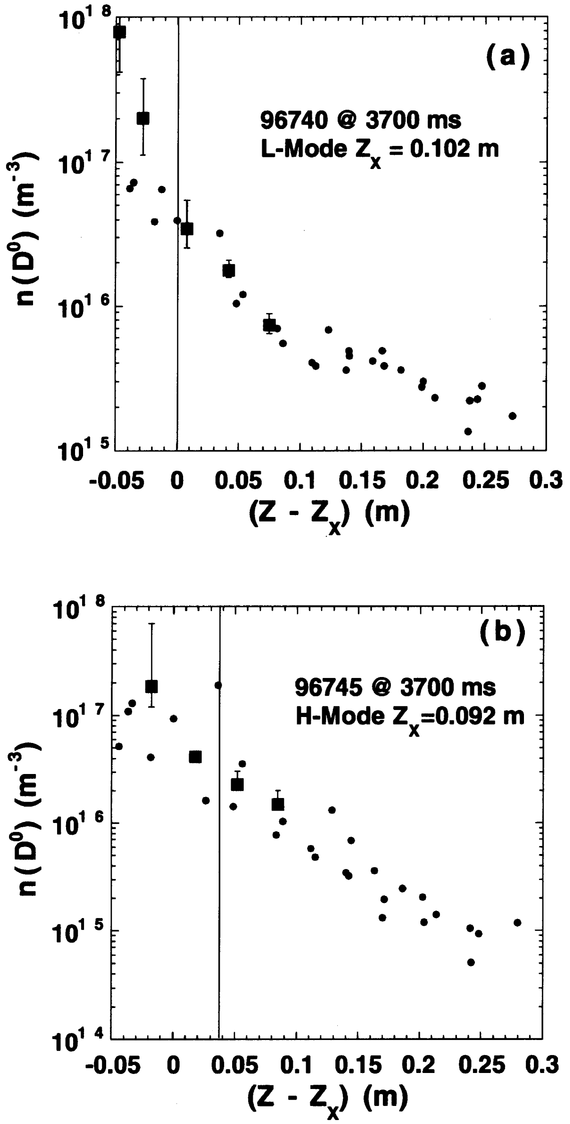

Fig. 3. Measured X-point neutral densities, $n(D^0)$, (solid squares) are higher in H-mode than in L-mode. Both L-mode (a) and H-mode (b) data are well reproduced by the model calculations (solid circles). A calculated neutral density is shown for each grid cell whose centroid is radially within 0.05 m of the DTS chord.

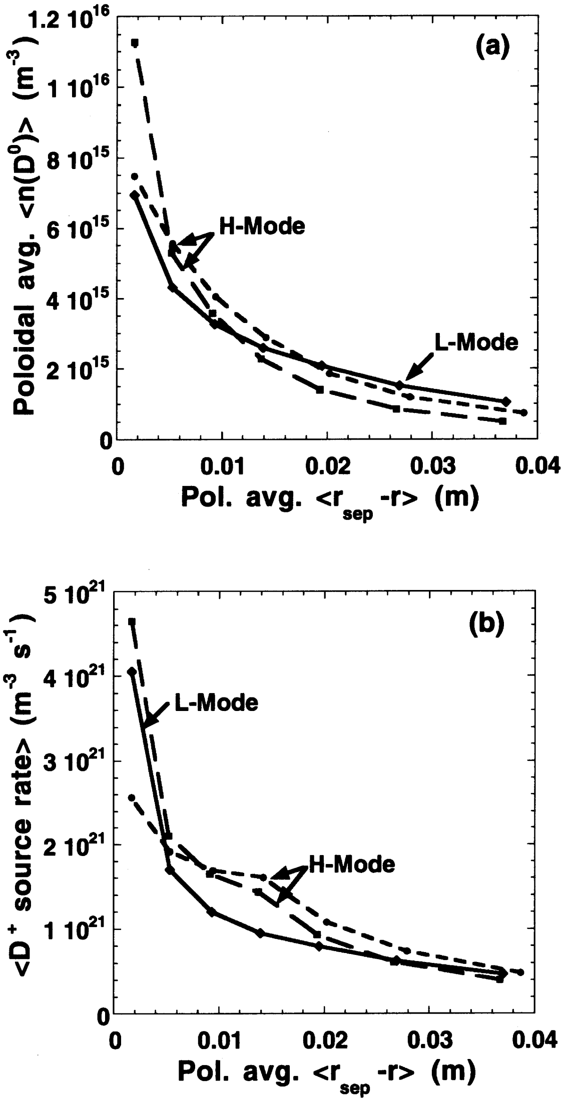

Fig. 4. Poloidally averaged neutral density (a) and core ion source rate (b) are shown for L- and H-mode plasmas as functions of average distance from the separatrix. Effects of the pedestal are evident in the flattening of H-mode profiles.

larger than that in L-mode; this is a general result for the discharges analyzed here. The model is seen to reproduce the measured deuterium atomic neutral density, $n(D^0)$, quite well for both confinement modes in both magnitude and scale length. This leads to significantly greater confidence in the accuracy of the calculated core fueling rates and particle confinement times than would be the case if the $n(D^0)$ data were not available.

4. Discussion and conclusions

Agreement of the core fueling rate from DEGAS with the integrated particle flux crossing the separatrix, Γ_{core}, from B2.5 (determined from the core particle balance equation $dN_{core}/dt = \Gamma_{fuel} + \Gamma_{NBI} - \Gamma_{core}$) is the key requirement for establishing consistency of the plasma and neutral transport. Here Γ_{fuel} is the core fueling rate from divertor recycling and Γ_{NBI} is the beam fueling rate. The core plasma global particle confinement time is defined as $\tau_p = N_{core}/\Gamma_{core}$, where N_{core} is the total core electron number. As defined here τ_p is global in the sense that it is an average over the entire core plasma. The local particle confinement time as well as the core fueling rate are strongly dependent upon radius. The poloidally averaged neutral densities and ion source rates in the core of L- and H-mode plasmas are displayed in Figs. 4(a) and (b) as functions of the poloidally averaged distance inside the separatrix. The effect of the H-mode pedestal is seen as a flattening of the fueling profile at the pedestal. This effect is even more pronounced in the corresponding poloidally averaged charge-exchange rate (not shown).

Results of core fueling and global particle confinement time calculations, as well as several discharge parameters, are summarized in Table 1. Good agreement of the calculated incident power at the inner and outer divertor with data from the IRTV camera are also noted. That core particle balance is realized in these simulations is seen by summing the sources and sinks in the above equation. The comparison of global energy and particle confinement times indicates that in both L- and H-modes the particle confinement time is less than but within 50% of the energy confinement time. This result agrees with the conclusions reached in [11] by a different analysis technique. The confinement times are lower by factors of two to three than those deduced in [7,12].

An important result that emerges from this study is that core particle fueling stays relatively constant between L-mode and the ELM-free H-mode phase immediately following the L–H transition. This result, clearly seen in the DEGAS core fueling rates and the integrated divertor ion fluxes in Table 1, agrees with the conclusion reached in [13]. This indicates that in the ELM-free phase nearly all of the increase in plasma electron density comes from a decrease in the cross-field transport rate and an increase in the impurity influx, rather than from changes in the SOL plasma. Since, as we have shown for DIII-D, the core is fueled predominantly by recycling from the divertor plate and through the divertor plasma, it is perhaps not surprising that the thinner H-mode SOL would have less effect on core fueling than if the fueling were predominantly from limiters.

Acknowledgements

Research sponsored by the Office of Fusion Energy, US Department of Energy, under contract DE-AC05-00OR22725 with UT-Batelle LLC, DE-AC03-89ER51114 at General Atomics, and W-7405-ENG-48 at LLNL. Very useful discussions with B.A. Carreras and P.K. Mioduszewski on the neutrals issues are gratefully acknowledged. We thank Jon Watkins and Charles Lasnier for providing diagnostic data, and the DIII-D operations staff for their work in running the experiments.

References

[1] S.I. Itoh, K. Itoh, Nucl. Fus. 29 (1989) 1031.
[2] K.C. Shaing, C.T. Hsu, Phys. Plasmas 2 (1995) 1801.
[3] B.A. Carreras, P.H. Diamond, G. Vetoulis, Phys. Plasmas 3 (1996) 4106.
[4] F. Wagner, G. Becker, K. Behringer, et al., Phys. Rev. Lett. 49 (1982) 1408.
[5] B.A. Carreras, L.W. Owen, R. Maingi, P.K. Mioduszewski, T.N. Carlstrom, R.J. Groebner, Phys. Plasma 5 (1998) 2623.
[6] R.J. Colchin, R. Maingi, M.E. Fenstermacher, T.N. Carlstrom, L.W. Owen, R.C. Isler, Nucl. Fus. 40 (2000) 175.
[7] L.W. Owen, R. Maingi, D.K. Lee, P.K. Mioduszewski, D.R. Baker, D.L. Hillis, J.T. Hogan, G.L. Jackson, M.R. Wade, J. Nucl. Mater. 220–222 (1995) 315.
[8] B.J. Braams, Contribution Plasma Phys. 36 (1996) 276.
[9] D.B. Heifetz, D. Post, M. Petravic, J. Weisheit, G. Bateman, J. Comp. Phys. 46 (1982) 309–327.
[10] R. Maingi, J.T. Hogan, L.W. Owen, P.K. Mioduszewski, M.E. Rensink, J.G. Gilligan, O.E. Hankins, K.A. Werley, Nucl. Fus. 34 (1994) 283–287.
[11] G.D. Porter, DIII Team, Phys. Plasmas 5 (1998) 4311.
[12] M.E. Rensink, S.L. Allen, A.H. Futch, D.N. Hill, G.D. Porter, Phys. Fluids B 5 (1993) 2165.
[13] D.R. Baker, R. Maingi, L.W. Owen, G.D. Porter, G.L. Jackson, J. Nucl. Mater. 241–243 (1997) 602.